Peptide Models of Helical Hydrophobic Transmembrane Segments of Membrane Proteins. 1. Studies of the Conformation, Intrabilayer Orientation, and Amide Hydrogen Exchangeability of Ac-K_2-$(LA)_{12}$-K_2-amide†

Yuan-Peng Zhang,‡ Ruthven N. A. H. Lewis,‡ Gillian D. Henry,‡,§ Brian D. Sykes,‡,§ Robert S. Hodges,‡,§ and Ronald N. McElhaney*,‡

Department of Biochemistry and MRC Group in Protein Structure and Function, University of Alberta, Edmonton, Alberta, Canada, T6G 2H7

Received September 15, 1994⊗

ABSTRACT: The secondary structure, amide hydrogen exchangeability, and intramembrane orientation of the hydrophobic peptide Ac-K_2-$(LA)_{12}$-K_2-amide [$(LA)_{12}$] were studied by a combination of circular dichroism (CD), Fourier transform infrared (FTIR), and proton nuclear magnetic resonance (^{1}H NMR) spectroscopic techniques. All three techniques indicate that $(LA)_{12}$ adopts predominantly helical conformations in various organic solvents, detergent micelles, and phospholipid bilayers. Also, attenuated total reflectance FTIR studies of oriented phospholipid bilayers demonstrate that $(LA)_{12}$ is arranged with the long helical axis perpendicular to the bilayer plane. FTIR and ^{1}H NMR studies of the exchangeability of the amide protons of $(LA)_{12}$ indicate that in all media there are at least two populations of amide protons which exchange with the bulk solvent at markedly different rates. Moreover, the ^{1}H NMR spectroscopic studies indicate that, in organic solvents and micellar dispersions, amide proton exchange rates decrease progressively from the N- or C-terminus of the peptide toward the central region. Our results are thus consistent with $(LA)_{12}$ retaining a predominantly helical structure with so-called frayed ends in all media. The amide proton exchange studies also indicate that when $(LA)_{12}$ is dispersed in lipid bilayers, the slowly exchanging population of amide protons is larger than that observed in organic solvents or in micellar dispersions and that most of that proton population is virtually unexchangeable. Such observations are consistent with the sequestration of the central regions of the peptide in the hydrophobic domains of the lipid bilayer. The CD and FTIR data indicate that although $(LA)_{12}$ seems to retain conformations with a high α-helical content in all media examined, its conformation is sensitive to the composition of the surrounding medium, in contrast to the polyleucine-based analogues which have been studied previously. In particular, the FTIR spectroscopic data indicate that $(LA)_{12}$ may exhibit an amide I absorption band between 1633 and 1639 cm^{-1} under some circumstances. The relative intensity of this band changes with the composition of the surrounding medium and its appearance has previously been correlated with the formation of 3_{10}-helical structures [Miick *et al.* (1992) *Nature 359*, 653−655]. Thus $(LA)_{12}$ may be interconverting between different helical conformations in response to changes in the physical properties of the medium in which the peptide is dispersed. Our results suggest that $(LA)_{12}$ should serve as a good peptide model of hydrophobic, transmembrane helices which are conformationally sensitive to the properties of the lipid bilayer in which they reside.

The interactions between proteins and lipids are of fundamental importance to the structure and function of all biological membranes. Indeed, the secondary structure and the activity of many integral transmembrane proteins is modulated by the physical properties of the host lipid bilayer (Sandermann, 1978; McElhaney, 1982, 1995). To date, most of the data on lipid−protein interactions have been obtained from studies of natural membrane proteins in both natural and reconstituted membrane systems. However, an inherent problem with such studies is that natural integral membrane proteins are often large, multisubunit aggregates for which information on their three-dimensional structures and intramembrane topologies are unknown or incomplete. Moreover, many such proteins tend to interact with even a single species of membrane lipid in complex, multifaceted ways [for examples, see McElhaney (1986), and George *et al.* (1989, 1990)], resulting in data which can be difficult to interpret. Indeed, largely because of such problems, our current understanding of the molecular mechanisms of the interaction of hydrophobic transmembrane proteins and membrane lipids remains incomplete, despite the numerous studies of lipid−protein interactions that have been performed so far [for reviews, see Watts and De Pont (1985, 1986), Cserhåti and Szogyi (1991, 1992, 1993, 1994), Epand and Epand (1992), and Selinsky, (1992)].

To circumvent the problems outlined above, current approaches to the study of lipid−protein interactions tend to employ peptide models which are designed to interact specifically with either the polar, the interfacial, or the hydrophobic domains of lipid bilayers [for examples, see Jacobs and White (1986, 1987), Mclean *et al.* (1991), Davis

† This work was supported by operating and major equipment grants from the Medical Research Council of Canada and by major equipment grants from the Alberta Heritage Foundation for Medical Research.
* Author to whom correspondence should be addressed.
‡ Department of Biochemistry.
§ MRC Group in Protein Structure and Function.
⊗ Abstract published in *Advance ACS Abstracts,* February 1, 1995.

0006-2960/95/0434-2348$09.00/0

et al. (1983), Huschilt *et al.* (1985, 1989), Morrow *et al.* (1985) Pauls *et al.* (1985), and Roux *et al.* (1989)]. This approach has been successfully used by others and ourselves to model the interaction of helical hydrophobic transmembrane proteins with lipid bilayers (Davis *et al.*, 1983; Huschilt *et al.*, 1985, 1989; Morrow *et al.*, 1985; Pauls *et al.*, 1985; Roux *et al.*, 1989; Zhang *et al.*, 1992a,b, 1995a). The peptide models used in these studies (Ac-K_2-G-L_n-K_2-A-amide) consist of a long sequence (16−24 residues) of hydrophobic leucine residues capped at both the N- and the C-termini with two polar lysine residues. These peptides (P_{16} and P_{24})[1] were designed to spontaneously form hydrophobic α-helices which partition into the hydrophobic domain of lipid bilayers with their charged lysine terminal residues located at or near to the bilayer polar headgroups or polar/apolar interfacial regions. Studies of these peptide models have demonstrated that they do form very stable α-helices (Davis *et al.*, 1983; Zhang *et al.*, 1992a), traverse the hydrophobic domains of hydrated PC and PE bilayers (Davis *et al.*, 1983; Morrow *et al.*, 1985, Roux *et al.*, 1989; Zhang *et al.*, 1992a,b, 1995a), and insert into lipid bilayers with the long axis of the peptide helix more or less perpendicular to the bilayer surface (Huschilt *et al.*, 1989). Indeed, these peptides appear to interact primarily with the hydrocarbon chains of PC and PE bilayers and can be considered typical class III (i.e., integral, transmembrane) peptides or proteins, as first defined by Papahadjoupoulos *et al.* (1975) and later refined by McElhaney (1986).

The P_{24} peptide model of hydrophobic transmembrane α-helical segments of integral membrane proteins has been very useful in examining the nature of lipid−peptide interactions that are likely to occur when there is a mismatch between bilayer hydrophobic thickness and the hydrophobic length of the transmembrane α-helix. Recent studies of the interaction of this peptide with PC and PE bilayers have shown that the structural adjustments to a mismatching of hydrophobic length mainly involve changes in the conformational disorder of the lipid hydrocarbon chains at small to moderate degrees of mismatch and lipid/peptide phase separation when the hydrophobic mismatch becomes significantly large (Zhang *et al.*, 1992b, 1995a). Interestingly, however, such studies also suggest that mismatching of peptide hydrophobic length and bilayer hydrophobic thickness can result in structural alterations of the peptide. With the P_{24} peptide model, only small distortions of the peptide helix were detected, presumably because its α-helical structure is extraordinarily stable. Nevertheless, the fact that changes in structure of the peptide were detected is significant, since it suggests a possible mechanism whereby changes in the degree of conformational disorder of lipid bilayers can be transmitted to proteins which are guests within those bilayers. To investigate this aspect of lipid−protein interactions further, we have begun a study of the interactions of lipids with model peptide hydrophobic helices which are designed to be less stable than P_{24}. The peptide model used in these studies, $(LA)_{12}$, is conceptually similar to P_{24} and like the latter is designed to form hydrophobic transmembrane helices that will partition into lipid bilayers with their long axis perpendicular to the bilayer surface and their charged termini anchored at the bilayer surface. However, because one half of the leucine residues of P_{24} has been replaced with alanine (an α-helical-forming amino acid with a smaller and much less hydrophobic side chain), $(LA)_{12}$ would be expected to form less stable and potentially more distortable helices which may be more conformationally sensitive to the properties of its host lipid bilayer. In this paper we present the results of our CD, FTIR, and ^{1}H NMR spectroscopic studies of the conformation of this model peptide $(LA)_{12}$ in organic solvents, detergent micelles, and lipid bilayers. We also present the results of our ATR-FTIR spectroscopic studies of the orientation of $(LA)_{12}$ in oriented phospholipid bilayers.

MATERIALS AND METHODS

Peptide Synthesis and Purification. The peptides $(LA)_{12}$ and L_{24} were synthesized using an Applied Biosystems 430A solid-phase peptide synthesizer (Foster City, CA). All amino acids precursors used for the synthesis were protected at the α-amino position with the *tert*-butyloxycarbonyl (Boc-) group (Bachem, Philadelphia, PA). In addition, the ϵ-amino side chains of the lysine derivative were protected with the (2-chlorobenzyl)oxycarbonyl group. All amino acids were double coupled using dicyclohexylcarbodiimide-generated symmetric anhydrides in DMF for the first coupling and in DCM for the second coupling to co-poly(styrene, 1% divinylbenzene)benzhydrylamine hydrochloride resin at a substitution of 0.9 mmol of NH_2 per gram of resin (Bachem, Philadelphia, PA). Any incomplete couplings (i.e., ≤99.2% coupling as determined by quantitative ninhydrin tests) were manually coupled a third time in *N*-methylpyrrolidone using a molar ratio of 2:2:2:3:1 of Boc-amino acids/2-(1H-benzotriazol-1-yl)-1,1,3,3-tetramethyluronium hexafluorophosphate/1-hydroxybenzotriazole/4-methylmorpholine/active sites on resin. The following steps were performed in the reaction vessel for each double coupling: (1) deprotection of the Boc-group with 33% TFA in DCM for 80 s; (2) 50% TFA in DCM for 18 min; (3) three DCM washes; (4) 10% DIEA in DMF 1 min; (5) 10% DIEA in DMF 1 min; (6) five DMF washes; (7) first coupling 30 min; (8) three DMF washes; (9) 10% DIEA in DMF for 45 s; (10) one DMF wash; (11) three DCM washes; (12) second coupling period 30 min; (13) one DMF wash; and (14) five DCM washes. Final acetylation was performed on the instrument using acetic anhydride/DIEA/mmol of peptide resin 50:20:1 for 10 min then 100:20:1 for 5 min in DCM. The completed peptides were cleaved from the resins with anhydrous hydrogen fluoride (20 mL/g of peptide resin) in the presence of 10% anisole and 1% ethanedithiol for 1 h at −4 °C using type 1B HF-Reaction Apparatus (Peninsula Laboratories Inc., Belmont, CA). The peptide−resin was then extracted three times with diethyl ether (25 mL each). The cleaved peptide

[1] Abbreviations: $(LA)_{12}$, Ac-K_2-$(LA)_{12}$-K_2-amide; P_{24}, Ac-K_2-G-L_{24}-A-K_2-amide; P_{16}, Ac-K_2-G-L_{16}-A-K_2-amide; L_{24}, Ac-K_2-L_{24}-K_2-amide; PC, phosphatidylcholine; PE, phosphatidylethanolamine; DPPC, dipalmitoylphosphatidylcholine; 16:0-lyso-PC, 1-*O*-palmitoyllysophosphatidylcholine; TFA, trifluoroacetic acid or trifluoroacetate; TFE, trifluoroethanol; DMF; dimethylformamide; DIEA diisopropylethylamine; DCM dichloromethane; FTIR, Fourier transform infrared; ATR, attenuated total reflectance; ATR-IR, attenuated total reflectance infrared; CD, circular dichroism; NMR, nuclear magnetic resonance; TOCSY, total correlation spectroscopy; NOE, nuclear Overhauser effect; NOESY, nuclear Overhauser effect spectroscopy (two dimensional); R_p, mole fraction of peptide in a peptide/lipid mixture. The hydrocarbon chains of the lipids used in this study are designated by the shorthand notation *N*:0 with "*N*" representing the number of carbon atoms on the chain and "0" indicating the absence of carbon−carbon double bonds.

was extracted from the resin with neat acetic acid (three times 25 mL each) and then lyophilized.

The peptides were subsequently purified from the crude extract as follows. The extract was first dispersed in 25% acetonitrile/75% water (80 mg/5 mL) and sonicated for 10 min while neat acetic acid was added dropwise until the sample cleared (5−10% acetic acid). The samples were then centrifuged to remove particulate matter (2 min at 14 000 rpm in an Eppendorf centrifuge 5414C) and subsequently syringe filtered using a Millex-6V 0.22 μm filter unit (Millipore, Bedford, MA). This solution was then purified by reversed-phase chromatography using an Applied Biosystems 400 solvent delivery system and a 783A programmable absorbance detector connected to a Synchropak RP-4 (250 × 21.2 mm i.d.) reversed-phase column (Synchrom Inc., Lafayette, IN) operating at a flow rate of 5 mL/min. The following linear AB gradient was used for purification: solvent A = 0.5% TFA/H_2O; B = 0.5% TFA/isopropanol. At time = 0, A = 80%, B = 20%; at time 300 min A = 20%, B = 80% (gradient rate 0.2% B/min). The fractions were then analyzed using a HP1090 liquid chromatograph (Hewlett Packard, Avondale, PA) using the above solvent system at 2% B/min starting in 100% solvent A on a Zorbax R_x-C8 2.1 mm × 15 cm column (Rockland Technologies, Giberstville, PA). The homogeneity of the purified peptide was determined by reversed-phase chromatography, amino acid analysis using a Beckman 6300 high performance analyzer (Allendale, NJ), and mass spectrometry using a BioIon 20 plasma desorption time-of-flight mass spectrometer (Uppsala, Sweden). Finally, the pure peptide was then twice lyophilized from 10 mM hydrochloric acid to replace the bound TFA counterions by chloride ions. This step was essential in the case of the FTIR spectroscopic samples because the strong C=O stretching band of the TFA group ($\cong$1670 cm^{-1}) overlaps with both the ester C=O stretching band of the lipid and the amide I band of the peptide (Surewicz & Mantsch, 1989).

Lipids and Other Materials. DPPC was synthesized and purified as previously described (Lewis *et al.*, 1987). Sodium dodecyl sulfate (specially purified for biochemical work) was obtained from BDH Chemicals Ltd. (Poole, England); 1-*O*-palmitoyllysophosphatidylcholine was obtained from Avanti Polar Lipids (Alabaster, AL); deuterium oxide (D_2O) was obtained from Aldrich (Milwaukee, WI) and was redistilled before use; methanol (CH_3OH) and deuterated methanol (CH_3OD) were from Aldrich; and perdeuterated methanol (CD_3OD) was obtained from MSD isotopes (Montreal, Quebec). All other solvents were of at least analytical grade quality and were redistilled before use.

Transmission FTIR Spectroscopy. Solid films of $(LA)_{12}$ were prepared for spectroscopy by drying from the appropriate solvents and analyzed by FTIR spectroscopy by the same methods described by Zhang *et al.* (1992a). Solution spectra of $(LA)_{12}$ dissolved in CH_3OH and in CH_3OD were recorded at high (7−10 mg/mL) and at low ($\cong$1.5 mg/mL) peptide concentrations using heatable demountable liquid cells equipped with thin (25 μm) and thick (0.1 mm) teflon spacers, respectively. Spectra of $(LA)_{12}$ in SDS micelles and in 16:0 lyso-PC micelles, and $(LA)_{12}$ dispersed in PC bilayers, were recorded using heatable demountable liquid cells equipped with 25 μm spacers. The SDS and 16:0 lyso-PC micellar solutions of $(LA)_{12}$ were prepared by dissolving the peptide in D_2O solutions of SDS (6% by wt) or 16:0-lyso PC (15 mg/mL) to obtain peptide concentration of 1.5 mg/mL. The PC-dispersed peptide mixtures were prepared for FTIR spectroscopy as follows: 2−3 mg of the lipid was codissolved with the peptide in methanol at the required lipid-to-peptide ratio and the solvent subsequently removed with a stream of nitrogen. After overnight evacuation to remove the last traces of solvent, the sample was hydrated with D_2O as described previously (Zhang *et al.*, 1992a, 1995a) and squeezed between the BaF_2 windows of a heatable, demountable liquid cell to form a 25 μm film. Once mounted in the sample holder of the instrument, the sample temperature could be controlled (between −20 and 90 °C) by an external, computer-controlled circulating water bath. Samples destined for proton/deuterum exchange experiments were dissolved in the appropriate deuterated solvent at room temperature and introduced into the FTIR instrument as quickly as possible. Typically the time interval between the initial exposure of the peptide to the deuterated solvent and the recording of the first spectrum was 5 min. The infrared spectra were recorded with a Digilab FTS-40 infrared spectrometer (Cambridge, MA) using the acquisition parameters previously described by Mantsch *et al.* (1985). The spectra obtained were corrected for solvent and/or water vapor absorption by the subtraction of appropriate reference spectra and analyzed using software supplied by Digilab Inc. and other computer programs obtained from the National Research Council of Canada. In cases where absorption bands were clearly definable in terms of a summation of component bands, Fourier self-deconvolution was used to obtain accurate estimates of the peak frequencies of the component bands, and curve-fitting procedures were subsequently used to obtain estimates of the widths and integrated areas of the component bands by reconstructing the contours of the original absorption band. The latter was achieved by a linear combination of the component bands identified by Fourier self-deconvolution with the aid of standard nonlinear least-squares minimization procedures. Each band was simulated by a Gaussian−Lorentzian function for which best fit estimates of band shape were achieved with approximately 70% Gaussian contribution. Under the conditions of these experiments, band narrowing factors up to 2.2 could be used during Fourier self-deconvolution without introducing significant distortions into the deconvolved spectra.

ATR-FTIR Spectroscopy. ATR-FTIR spectra were acquired with a Digilab FTS-60 spectrometer equipped with a Wilmad overhead ATR accessory (Wilmad Glass Co, Buena, NJ) and a grid polarizer (Cambridge Optics, Cambridge, MA) which was located between the sample and the detector. Oriented films of the lipid/peptide mixtures were spread on the surface of a zinc selenide ATR crystal (angle of incidence = 45°) as follows. Lipid/peptide mixtures of known R_p were codissolved in chloroform/methanol (2:1, v/v) at a lipid concentration of 0.1−0.2 mg/mL. Next, a few drops of the dilute solution so obtained were spread on the surface of the zinc selenide crystal and oriented by being gently rubbed with a teflon bar as the solvent slowly evaporated. Subsequently, the last traces of solvent were removed *in vacuo*. Hydration of the lipid/peptide films was achieved by saturating the atmosphere around the lipid/peptide film with D_2O vapor followed by repeated heating and cooling of the film through the temperature range of the gel/liquid-crystalline phase transition of the lipid. Saturation of the atmosphere around the lipid with D_2O vapor was achieved by sealing a

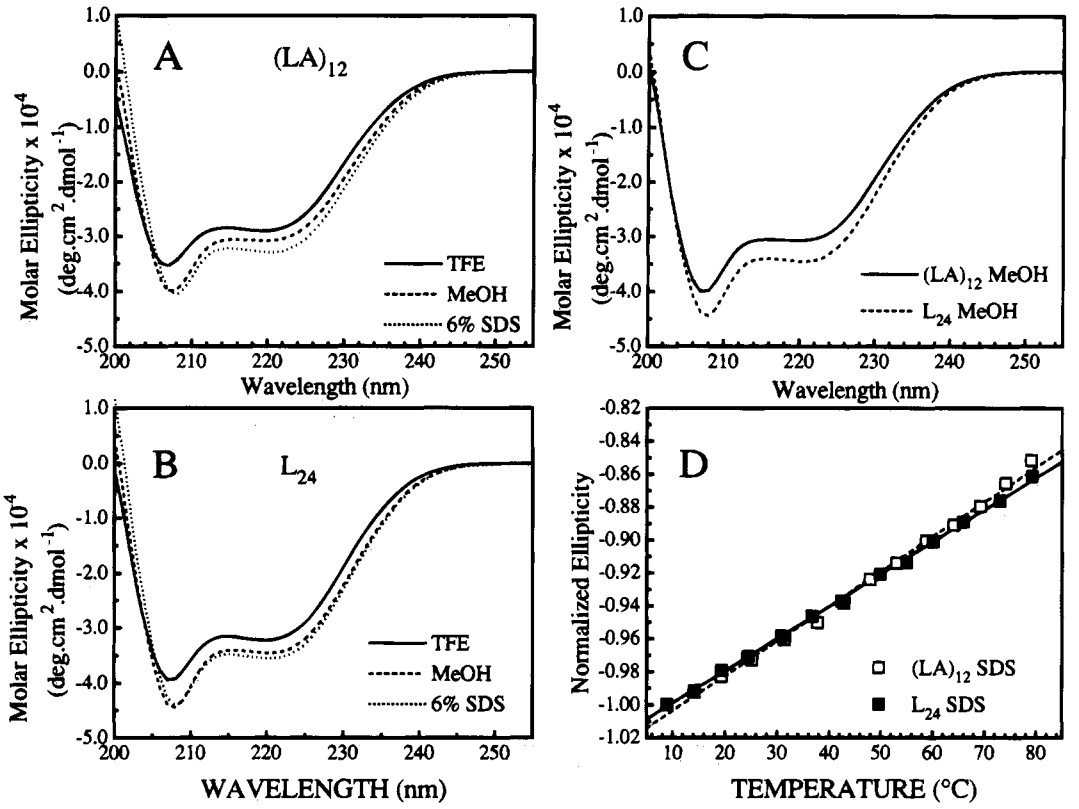

FIGURE 1: Comparative circular dichroism studies of the peptides $(LA)_{12}$ and L_{24}. (A) CD spectra of $(LA)_{12}$ in the various solvents. (B) CD spectra of L_{24} in the various solvents. (C) A comparison of the CD spectra of $(LA)_{12}$ and L_{24} in methanol. (D) Comparison of the temperature dependences of the molar ellipticities of $(LA)_{12}$ and L_{24} in SDS micelles. Ellipticities measured at 8 °C were assigned a value of −1, and all other values were normalized against this value.

piece of D_2O-soaked filter paper within the sample compartment of the heat exchange block used to control the temperature of the crystal. The D_2O-soaked filter paper served as a solvent reservoir and was carefully mounted such that it did not come in contact with the lipid/peptide film. That full hydration of the sample occurred under such experimental condition was verified by the magnitude of the D_2O absorptions in the IR spectra obtained and by the fact that the gel/liquid-crystalline phase transitions of the lipids were similar to those reported by DSC in the presence of excess water. Data were recorded and processed as described for transmission FTIR spectroscopy above.

^1H NMR Spectroscopy. NMR spectra of solutions of $(LA)_{12}$ in CD_3OH, CD_3OD and of dispersions in perdeuterated SDS micelles in H_2O and D_2O were acquired at 25 °C on a Varian Unity spectrometer (Palo Alto, CA) operating at 500 MHz. The nominal pH of the methanolic and aqueous solutions/dispersions of $(LA)_{12}$ was between 4.5 and 5. When spectra were recorded in CD_3OH or in H_2O, the solvent protons were suppressed by either the 1−1 pulse sequence to avoid solvent excitation (Hore, 1983) or by solvent presaturation (2.0 s) methods. For the two-dimensional experiments, quadrature detection employed the hypercomplex method of States *et al.* (1982), and 256−350 increments were typically collected. The final data matrix was zero-filled to 2048 data points. TOCSY spectra [see Bax and Davis (1985)] were recorded with a 70 ms mixing time (1 ms trim pulse, 60° final pulse). NOESY spectra were acquired using mixing times of 200 and 500 ms. Chemical shifts are referenced with respect to residual protons of the methyl group of methanol-d_3 at 3.31 ppm.

Circular Dichroism. Circular dichroism spectra were recorded at 20 °C on a Jasco J-500C spectropolarimeter (Jasco, Easton, MD) interfaced to an IBM PS/2 computer via a Jasco IF500II interface. The instrument was routinely calibrated with an aqueous solution of recrystallized d_{10}-(+)-camphorsulfonic acid. The data were collected at 0.1 nm resolution with a scan speed of 50 nm/min from 250 to 190 nm. Peptide concentrations (≅1.5 mg/mL) were determined by amino acid analysis.

RESULTS

Conformational Studies of Ac-$K_2(LA)_{12}K_2$-amide. The results of far ultraviolet CD studies of $(LA)_{12}$ in methanolic solution, TFE solution, and SDS micelles (6% aqueous SDS) are summarized in Figure 1. To enable more effective comparison between the properties of $(LA)_{12}$ and those of previously studied polyleucine-based peptides such as P_{24}, data from parallel studies of the polyleucine-based analogue L_{24} are also shown. The contours of the CD spectra of the two peptides are consistent with their adopting predominantly helical conformations in all of the solvents tested. Indeed, at 220 nm the observed molar ellipticity values (32 000−35 000) recorded at 8 °C are near the theoretical maximum (33 000) expected of a completely helical protein/peptide with the same number of amino acid residues [see Chen *et al.* (1974), and Chang *et al.* (1978) and references cited therein]. Comparable ranges of molar ellipticity values were obtained even when methanolic and TFE solutions of $(LA)_{12}$ were diluted with an equal volume of water (data not shown).[2] We also find that the ellipticities of both peptides decrease modestly with increasing temperature (see Figure

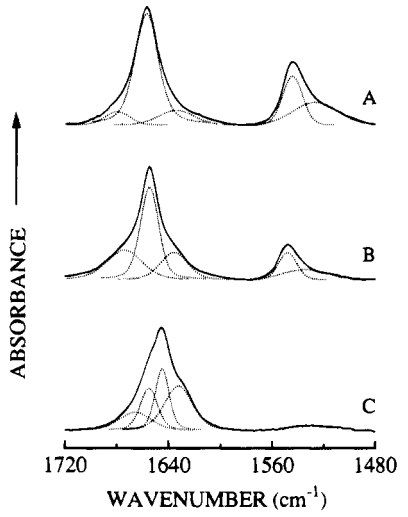

FIGURE 2: Amide I and amide II absorption bands of the infrared spectra of $(LA)_{12}$: (A) CH_3OH-dried film. (B) CH_3OH solution. (C) CH_3OD solution. The contours of the observed spectra are represented by the solid lines, and the dotted lines represent our estimates of the contours of the component bands as obtained by a combination of Fourier deconvolution and curve fitting. The data on the subcomponent bands are listed in Table 1.

1D). With both peptides these temperature-dependent decreases in ellipticity are thermally reversible, and although the magnitudes of these changes observed with the two peptides are generally similar (see Figure 1D), they do vary with the nature of the solvent used (TFE > MeOH > 6% SDS..., data not shown). Nevertheless, the observed thermally induced changes in ellipticity remain small (≅10−25% decrease over a 70 °C temperature range) under all conditions tested. However, a consistent feature of these measurements is that the molar ellipticities determined for $(LA)_{12}$ are always smaller than those of L_{24} under nominally identical conditions (see Figure 1C). Thus, although both peptides are predominantly helical under all experimental conditions tested, $(LA)_{12}$ may exhibit a somewhat smaller propensity to form helical structures. This possibility was further explored in our FTIR spectroscopic studies.

Illustrated in Figure 2 are the amide II (≅1545 cm^{-1}) and conformationally sensitive amide I (≅1655 cm^{-1}) absorption bands obtained from methanol-dried $(LA)_{12}$ films and from solutions of $(LA)_{12}$ in CH_3OH and in CH_3OD. The amide I and amide II absorption bands of all these spectra are resolvable into subcomponents, which arise from amide I vibrations of different conformational domains of the peptide and from the A and E_1 symmetry species of the amide II vibration, respectively (Chirgadze & Brazhnikov, 1976; Sengupta & Krimm, 1985). Information on the conformational disposition of $(LA)_{12}$ was deduced from the components of the amide I absorption band as summarized in Table 1. For solid films dried from CH_3OH (or from TFE) solutions of $(LA)_{12}$ (Figure 2A), the amide I band can be resolved into components which are centered near 1680, 1657, and 1634 cm^{-1}. The absorption band near 1657 cm^{-1} is the most intense (≅75% total integrated intensity) and can be assigned to amide I vibrations arising from the α-helical domains of the peptide (Miyazawa & Blout, 1961). The components centered near 1634 and 1680 cm^{-1}, which

[2] Comparable measurements were not made with L_{24} because it is insoluble under those conditions.

Table 1: Estimates of the Subcomponents of the Amide I Absorption Band of $(LA)_{12}$ Dispersed or Dissolved in Various Media

band maximum (cm^{-1})	half width (cm^{-1})	area (% total)	comments
	CH_3OH-Dried Film		
1634	31	16	
1657	21	74	α-helix
1680	22	10	
	TFE-Dried Film		
1636	36	20	
1658	24	70	α-helix
1682	21	10	
	CH_3OH Solution		
1638	19	27	
1655	16	39	α-helix
1672	30	34	
	CH_3OD Solution		
1633	22	27	
1647	16	34	α-helix, D-bonded
1656	16	19	α-helix, H-bonded
1668	24	20	
	CH_3OD/D_2O (1:1, v/v) Solution		
1637	26	41	
1648	14	26	α-helix, D-bonded
1655	14	20	α-helix, H-bonded
1662	17	13	
	D_2O Dispersion		
1633	29	40	
1647	16	10	α-helix, D-bonded
1656	18	30	α-helix, H-bonded
1667	15	20	
	SDS Micelles in D_2O		
1633	19	14	
1645	15	32	α-helix, D-bonded
1655	13	42	α-helix, H-bonded
1664	19	12	
	16:0 Lyso-PC Dispersion in D_2O (40 °C)		
1636	25	35	
1646	14	21	α-helix, D-bonded
1655	13	30	α-helix, H-bonded
1665	19	14	
	16:0 Lyso-PC Dispersion in D_2O (−10 °C)		
1633	25	54	
1646	14	21	α-helix, D-bonded
1654	14	17	α-helix, H-bonded
1664	23	14	
	DPPC Bilayers Hydrated with D_2O (50 °C)		
1637	22	17	
1649	16	28	α-helix, D-bonded
1658	13	40	α-helix, H-bonded
1668	20	15	

together comprise some 25% of the total integrated intensity of the amide I absorption band, are thought to arise from non α-helical (but not necessarily nonhelical) domains of the peptide. In CH_3OH solution (Figure 2B) the distribution of integrated intensity between these three components changes significantly. When compared with the solid films, the contributions of both the high- and low-frequency components to the integrated intensity of the amide I band increase significantly at the obvious expense of the 1657 cm^{-1} component (see Figure 2B and Table 1), suggesting that there is a substantial decrease in α-helical content when $(LA)_{12}$ dissolves in methanol. A similar conclusion was drawn from our studies of the FTIR spectrum of $(LA)_{12}$ in CH_3OD. In the deuterated solvent, spectra of superior quality

were obtained because of the weaker background of solvent absorption. However, in this case the contours of the amide I absorption band differ from those observed in CH_3OH solution because of the effects of H/D exchange. The latter was manifest by the diminution in the integrated intensity of the amide II band and shifts in the peak frequencies of some components of the amide I band (Chirgadze & Brazhnikov, 1976; Rabolt *et al.*, 1977; Dwivedi & Krimm, 1984). As illustrated in Figure 2C, the amide I band of $(LA)_{12}$ dissolved in CH_3OD is resolvable into four components centered near 1668, 1655, 1645, and 1633 cm^{-1} (see Figure 2C and Table 1). The components centered near 1655 and 1645 cm^{-1} are attributable to the amide I absorption bands of protonated and deuterated α-helical domains of the peptide, respectively (Chirgadze & Brazhnikov, 1976; Rabolt *et al.*, 1977; Dwivedi & Krimm, 1984), and, as was observed in CH_3OH solution, these bands together account for approximately 50% of the total integrated intensity of the amide I absorption band. It is noteworthy that the observations noted above differ markedly from similar studies of the model peptide P_{24}, for which the integrated intensity of the amide I absorptions assigned to α-helical structures account for at least 70% of the total integrated intensity under all conditions observed (Zhang *et al.*, 1992a). Presumably this is because the α-helical domains of P_{24} are more conformationally stable with respect to other helical or nonhelical structures than are those of $(LA)_{12}$. Another significant feature of the data presented above is our spectroscopic evidence that although significant proportions of α-helical structures are always present, they may not always be predominant when $(LA)_{12}$ dissolves in organic solvents. This result is particularly interesting given that our CD studies (see above) and NMR spectroscopic data (see below) both indicate that $(LA)_{12}$ is predominantly helical under those conditions. This apparent difference in results is not due to differences in the peptide concentrations typically used for CD and NMR spectroscopy (1−5 mg/mL) and for FTIR spectroscopy (7−10 mg/mL), because the distribution of the integrated intensity of the amide I band among the three subcomponents described above does not change when infrared spectra are recorded at concentrations typically used in CD and NMR spectroscopic experiments. If $(LA)_{12}$ is predominantly helical in organic solvents, then our FTIR spectroscopic evidence for the existence of significant amounts of non-α-helical structure in organic solvents suggests that $(LA)_{12}$ may be adopting helical conformations other than the more commonly observed α-helix. The suggestion that $(LA)_{12}$ may actually form smaller α-helical domains than do polyleucine-based analogues such as P_{24} has many interesting implications which will be explored further in the Discussion.

The amide I and amide II bands of the infrared spectra of $(LA)_{12}$ dispersed in aqueous SDS micelles, in aqueous 16:0 lyso-PC micelles, and in hydrated DPPC bilayers are presented in Figure 3. These studies were designed to examine the conformational sensitivity of $(LA)_{12}$ to its interaction with detergents and lipid bilayers. The spectra shown in Figure 3 were recorded in D_2O dispersions and as a result there is a diminution in the relative intensity of the amide II band because of H/D exchange. As illustrated in Figure 3, the amide I absorption bands of $(LA)_{12}$ in SDS or 16:0 lyso-PC micelles and in hydrated DPPC bilayers (spectra A, B, D, and E) are essentially similar. Under these

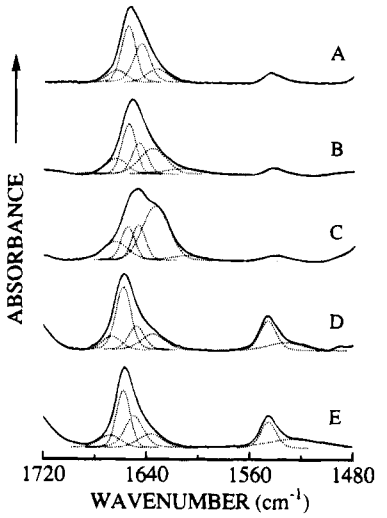

FIGURE 3: Amide I and amide II absorption bands of the infrared spectra of $(LA)_{12}$. (A) Dispersed in SDS micelles. (B) Dispersed in 16:0 lyso-PC at 40 °C. (C) Dispersed in 16:0 lyso-PC at −10 °C. (C) Dispersed in gel phase DPPC bilayers at 20 °C. (D) Dispersed in liquid-crystalline DPPC bilayers at 50 °C. The contours of the observed spectra are represented by the solid lines, and the dotted lines represent our estimates of the contours of the component bands as obtained by a combination of Fourier deconvolution and curve fitting. The data on the subcomponent bands are listed in Table 1.

conditions the contours of the amide I band are resolvable into four component bands which are centered near 1664, 1655, 1645, and 1633 cm^{-1} (see Figure 3C and Table 1). The components centered near 1655 and 1645 cm^{-1} can be attributed to amide I absorption bands arising from protonated and deuterated α-helical domains of the peptide (Chirgadze & Brazhnikov, 1976; Rabolt *et al.*, 1977; Dwivedi & Krimm, 1984), and, for dispersions in SDS or 16:0 lyso-PC micelles and DPPC bilayers, they comprise approximately 70% of the total integrated intensity of the $(LA)_{12}$ amide I absorption. These results are thus consistent with $(LA)_{12}$ adopting predominantly α-helical conformations when dispersed in these detergent or lipid assemblies. Interestingly, we also find that the contours of the $(LA)_{12}$ amide I absorption band change significantly when samples dispersed in 16:0 lyso-PC micelles are cooled to low temperatures (0 °C). Specifically, there is an increase in the intensity of the low frequency component (≅1633 cm^{-1}) at the obvious expense of the α-helical components of the amide absorption band (see Figure 3C and Table 1), and the contribution of this low-frequency component to the total area of the amide I band increases with further cooling of the sample. These thermally induced changes in the contours of the $(LA)_{12}$ amide I absorption are reversible and the discontinuous change in the intensity of the 1633 cm^{-1} band coincides with the coagel/micellar phase transition of aqueous 16:0 lyso-PC. Interestingly, such changes are not observed at the gel/liquid-crystalline phase transition of DPPC/$(LA)_{12}$ mixtures (see Figure 3, spectra D and E). Nevertheless, the above observations are significant because they provide evidence that the conformational disposition of $(LA)_{12}$ can be altered by structural changes in the lipid assemblies with which it interacts.

Studies of Amide Hydrogen Exchange in Ac-$K_2(LA)_{12}K_2$-amide. FTIR and NMR spectroscopy were used to study the exchangeability of the amide protons of $(LA)_{12}$ so as to examine the conformational stability of the peptide and its

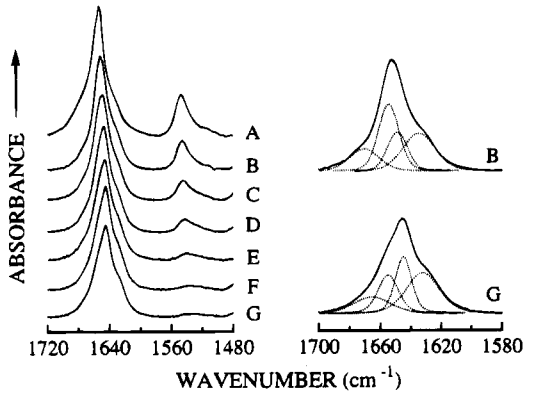

FIGURE 4: Amide I and amide II absorption bands of the infrared spectra of $(LA)_{12}$ observed in CH_3OD (left panel) at 30 °C. The spectra shown were obtained at various points during the H/D exchange as indicated below. The right panel shows the contours of the amide I band of two of these spectra. The observed spectra are represented by the solid lines, and the dotted lines represent our estimates of the contours of the component bands as obtained by a combination of Fourier deconvolution and curve fitting. (A) Unexchanged reference sample in CH_3OH. (B) Time = 5 min. (C) Time = 30 min. (D) Time = 75 min. (E) Time = 2.5 h. (F) Time = 5 h. (G) Time = 8 h.

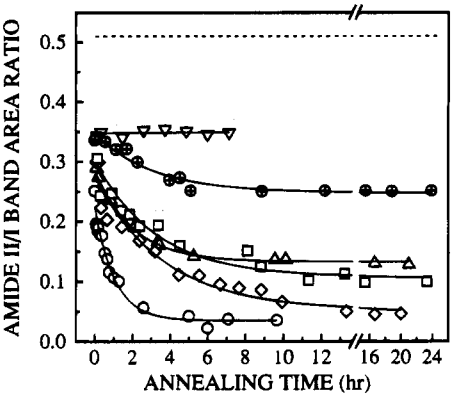

FIGURE 5: Time-dependent changes in the amide II/amide I intensity ratios of $(LA)_{12}$ dispersed or dissolved in various media. The dashed line indicates the magnitude of the intensity ratio observed with a CH_3OH dried film. (open circles) CH_3OD solution. (open triangles) Dispersed in D_2O. (open diamonds) Dispersed in 16:0-lyso PC. (open boxes) Dispersed in SDS. (circles with crosses) Dispersed in liquid crystalline DPPC bilayers. (inverted open triangles) Dispersed in gel phase DPPC bilayers.

exposure to the solvent when dispersed or dissolved in the various media. Figure 4 shows time-dependent changes in the contours of the amide I and amide II absorption bands in the infrared spectrum of a CH_3OD solution of $(LA)_{12}$ at 30 °C. As expected, H/D exchange of the amide hydrogens is accompanied by changes in contours of both the amide I and amide II absorption bands. In the amide I region H/D exchange is manifest by a progressive growth of an absorption band near 1645 cm^{-1} in concert with a proportional decrease in the intensity of the absorption band near 1655 cm^{-1}. These two bands arise from the stretching vibrations of deuterium-bonded ($\cong$1645 cm^{-1}) and hydrogen-bonded ($\cong$1655 cm^{-1}) amide carbonyl groups within α-helical domains of peptides or proteins [see Chirgadze and Brazhnikov (1976), Rabolt *et al.* (1977), and Dwivedi and Krimm (1984)]. In the amide II region, H/D exchange is manifest by a progressive decrease in the intensity of the amide II band near 1545 cm^{-1}, primarily because N-deuteration of the amide hydrogens shifts the amide N−H/D bending absorption to lower frequencies. From the amide II regions of the spectra shown in Figure 4, it is evident that a large fraction of amide hydrogens can be exchanged under relatively mild conditions. In this respect $(LA)_{12}$ differs markedly from the polyleucine model peptide P_{24}, for which comparable levels of H/D exchange could only obtained under considerably harsher conditions (Zhang *et al.*, 1992a).

The rate of amide H/D exchange was semiquantitatively monitored by examining the amide II/amide I intensity ratios as a function of time. Irrespective of the environment in which $(LA)_{12}$ is dispersed or dissolved, there are at least two populations of amide hydrogens which exchange with the solvent at markedly different rates (see Figure 5). One population exchanges fairly quickly (half life $\cong$ seconds to minutes) whereas the other exchanges at a considerably slower rate (half life $\cong$ hours to days). Figures 4 and 5 also indicate that the relative sizes of the fast and slowly exchanging populations of amide protons depend upon the medium in which $(LA)_{12}$ is dissolved or dispersed. As shown in Figure 5, the population of slowly exchangeable amide protons observed when $(LA)_{12}$ is dispersed in DPPC appears to be larger than that observed when it is dispersed in aqueous SDS micelles, which in turn are larger than that observed when $(LA)_{12}$ is dissolved in methanolic solution. Interestingly, little or no H/D exchange is observed when $(LA)_{12}$ is initially dispersed in the gel phase of DPPC, and significant exchange is only observed when the sample is heated to temperatures above the gel/liquid-crystalline phase transition of the lipid. This observation may be indicative of differences in the exposure of potentially exchangeable amide protons of $(LA)_{12}$ in the thicker gel and thinner liquid-crystalline states of the lipid, and/or differences in the penetration of water into the interfaces of the gel and liquid-crystalline phases of the lipid/peptide mixture. Also, even when $(LA)_{12}$ is dispersed in water the size of the slowly exchanging population of amide protons appears to be only slightly larger than that observed when it is dispersed in aqueous detergent micelles (see Figure 5). That nontrivial amounts of amide hydrogen exchange occurs when $(LA)_{12}$ is dispersed in water seems remarkable given the fact that this peptide is insoluble in aqueous media. Interestingly, dispersal of $(LA)_{12}$ in water is also accompanied by significant changes in the contours of the amide I absorption band. When an aqueous dispersion of $(LA)_{12}$ is cooled to temperatures near 0 °C, the amide I component near 1636 cm^{-1} increases significantly and then decreases as the sample is cooled to temperatures where the water freezes. As illustrated in Figure 6, this spectroscopic change is remarkably similar to that which occurs when a micellar solution of $(LA)_{12}$ in 16:0 lyso-PC is cooled to low temperatures. These results, and the other H/D exchange data presented above, are undoubtedly attributable to changes in conformation and/or conformational stability of $(LA)_{12}$ when it is dispersed or dissolved in the various media examined, and to the effects of these media on the differential exposure of various regions of the peptide molecule to the solvent. However, more effective interpretation of the FTIR H/D exchange data requires some knowledge about the identity of the amino acids residues giving rise to these populations of differentially exchangeable amide protons as well as the location of these within the peptide molecule. This aspect of the structure of $(LA)_{12}$ was explored by ^1H NMR spectroscopy.

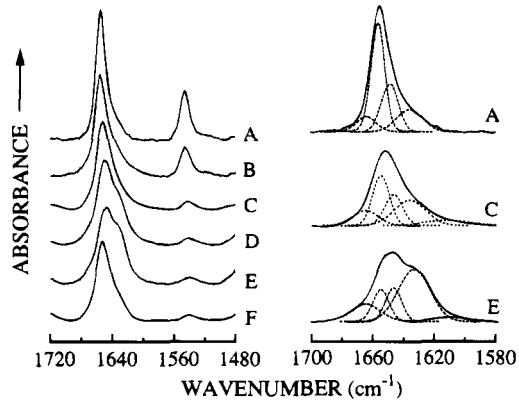

FIGURE 6: Amide I and amide II absorption bands of the infrared spectra of $(LA)_{12}$ observed in D_2O dispersion (left panel). The spectra shown were obtained at various points during the H/D exchange as indicated below. The right panel shows the contours of the amide I band of three of these spectra. The observed spectra are represented by the solid lines, and the dotted lines represent our estimates of the contours of the component bands as obtained by a combination of Fourier deconvolution and curve fitting. (A) $T = 40$ °C; time = 0.2 h. (B) $T = 40$ °C; time = 0.7 h. (C) $T = 40$ °C; time = 24 h. (D) $T = 10$ °C; time = 26 h. (E) $T = 0$ °C; time = 27 h. (F) $T = -15$°C; time = 28 h.

Illustrated in Figure 7 is the 500 MHz ^{1}H NMR spectrum of $(LA)_{12}$ in CD_3OH solution. The spectrum shown was obtained using solvent presaturation methods. Methanol is a convenient NMR solvent for hydrophobic peptides because much of its chemistry resembles that of water and peptides in methanolic solution typically form folded monomers which have short correlation times and narrow resonance lines, factors which are essential for obtaining high quality one- and two-dimensional spectra (Henry & Sykes, 1994). Also, many of the technical aspects of interpreting the hydrogen exchange data of peptides in methanolic solution have been addressed previously (Dempsey, 1988). As expected for a peptide of such restricted amino acid content, there is very little chemical shift dispersion among the α-proton and side chain resonances of $(LA)_{12}$. However, one of the structurally significant features of the NMR spectrum is that the chemical shifts of the resonances arising from the α-protons all occur between 4.00 and 4.25 ppm (labeled in Figure 7). α-Proton chemical shifts are excellent indicators of secondary structure, and those of $(LA)_{12}$ are all within the range for which strong statistical correlations with proteins/peptides in a helical configuration have been demonstrated (Wishart *et al.*, 1991). Unlike the α-protons, the amide protons of $(LA)_{12}$ resonate over a relatively broad range of frequencies (7.7−8.8 ppm). A number of these resonances are well resolved and exhibit the splitting attributable to spin−spin coupling. The spin−spin coupling constants of some of the well-resolved assigned resonances are listed in Table 2. In general, the spin−spin coupling constants ($^3J_{N\alpha}$) of the amide proton resonances are almost all small (<6 Hz). This feature is generally characteristic of proteins or peptides in helical conformations (Wüthrich, 1986). The observations noted above clearly suggest that the general features of the one-dimensional NMR spectrum are consistent with $(LA)_{12}$ being predominantly helical in methanolic solution.

The amide proton region of $(LA)_{12}$ obtained under varying conditions is shown in detail in Figure 7 (inset). It is clear that the spectrum acquired in CD_3OH solution using solvent presaturation methods is very similar to that obtained using the $1-\bar{1}$ pulse sequence (compare Figure 7, panels A and B). This shows that the peptide amide proton signals are not significantly diminished in intensity because of transfer of saturation from the solvent. However, the spectrum acquired with the $1-\bar{1}$ pulse sequence exhibits a broad

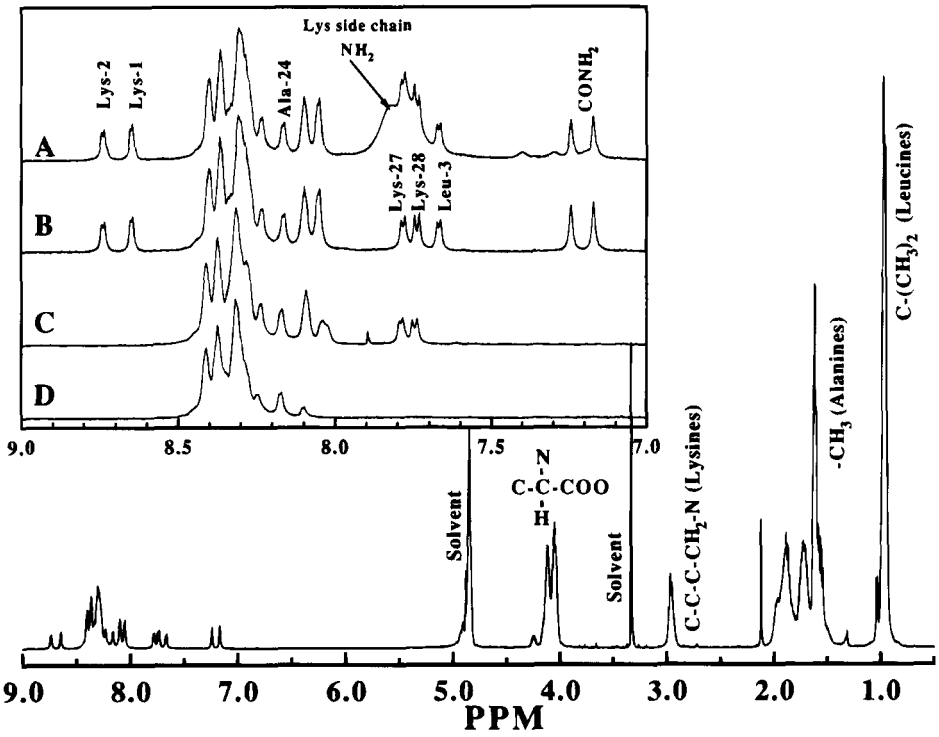

FIGURE 7: 500 MHz ^{1}H NMR spectrum of $(LA)_{12}$ in CD_3OH solution. The entire spectrum is shown at the bottom and was acquired using presaturation solvent suppression. The main groups of side chain resonances are as marked on the figure. The inset shows the amide proton resonances thus: (A) CD_3OH solution ($1-\bar{1}$ solvent suppression). (B) CD_3OH solution (presaturation solvent suppression). (C) CD_3OD solution (5 min after exposure to solvent). (D) CD_3OD solution (1 h after exposure to solvent).

Table 2: Assigned Amide Proton Resonances in the 500 MHz ^{1}H NMR Spectrum of Ac-$K_2(LA)_{12}K_2$-amide

chemical shift[a]	assignment	comments
7.24	$-CONH_2$	fast exchanging
7.17	$-CONH_2$	fast exchanging
7.67 (5.3)	Leu-3	fast exchanging
7.74 (7.7)	Lys-28	fast exchanging
7.79 (5.9)	Lys-27	fast exchanging
8.06	Ala-4; Leu-5	fast exchanging
8.10	Ala-26; Ala-6	fast exchanging
8.17	Ala-24	fast exchanging
8.24	Ala ??	slowly exchanging
8.25−8.30	Leu-25; other Leus	fast and slowly exchanging
8.31	alanines	slowly exchanging
8.37	leucines	slowly exchanging
8.41	leucines	slowly exchanging
8.65 (3.43)	Lys-1	fast exchanging
8.74 (4.39)	Lys-2	fast exchanging

[a] Chemical shifts are quoted in ppm. The coupling constants (Hz) are quoted in parentheses.

resonance at 7.7−7.8 ppm (see Figure 7A). The latter arises from the side chain amino protons of the lysine residues (confirmed in a TOCSY experiment). For these protons, amide hydrogen exchange rates with the solvent protons are sufficiently fast for saturation transfer to occur when the solvent is irradiated. The two upfield resonances at 7.24 and 7.17 ppm observed in spectra A and B arise from the primary amide protons of the C-terminal blocking group. The amide proton spectra of $(LA)_{12}$ acquired at 5 min and at 15 min after dissolution in perdeuterated methanol (CD_3OD) are also shown in Figure 7 (spectra C and D). A comparison with the spectra obtained in protonated solvent (spectrum B) enables one to identify resonances or groups of resonances arising from the rapidly and slowly exchanging populations observed in the infrared spectroscopic experiments. The slowly exchanging amides are clustered between 8.1 and 8.5 ppm, whereas the well-resolved resonances upfield and downfield of this range arise from the rapidly exchanging population. The spectra shown in Figure 7 also reveal that the exchange rates are not uniform within this group. For example, the two most downfield resonances (at 8.65 and 8.74 ppm) are completely exchanged within 5 min of exposure to perdeuterated methanol, whereas the resonances at 7.74 and 7.79 ppm are still detectable after 10−15 min. These observations are probably indicative of position-specific differential rates of amide hydrogen exchange under our experimental conditions. However, in the absence of information about the identity and the position of the amino acids residues giving rise to these and other resonances, a more detailed interpretation of the data cannot be made. Thus, two-dimensional NMR experiments were performed to identify amino acid residues giving rise to these various populations of amide protons and to obtain other information about the localization of these residues on the peptide.

The complete assignment of the ^{1}H resonances of a peptide with a repetitive amino acid sequence such as $(LA)_{12}$ is normally very difficult because of a high degree of resonance

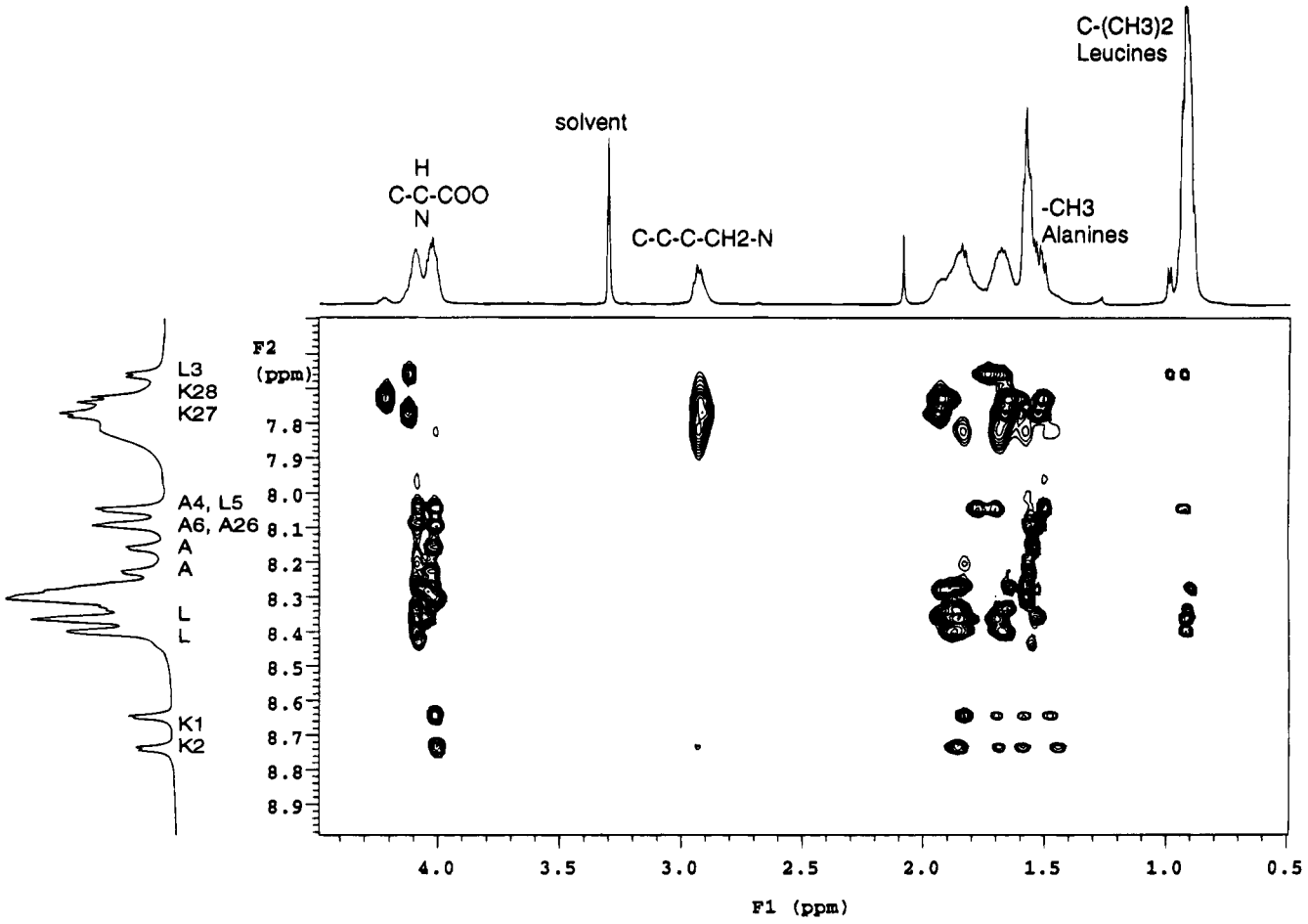

FIGURE 8: Two-dimensional NMR spectrum showing TOCSY connectivities between amide and the side chain resonances of $(LA)_{12}$. Amino acid residues giving rise to the amide resonances are as marked in the figure. The position specificities of the assigned resonances were determined in the NOESY experiment. Data were acquired in methanolic solution at 25 °C.

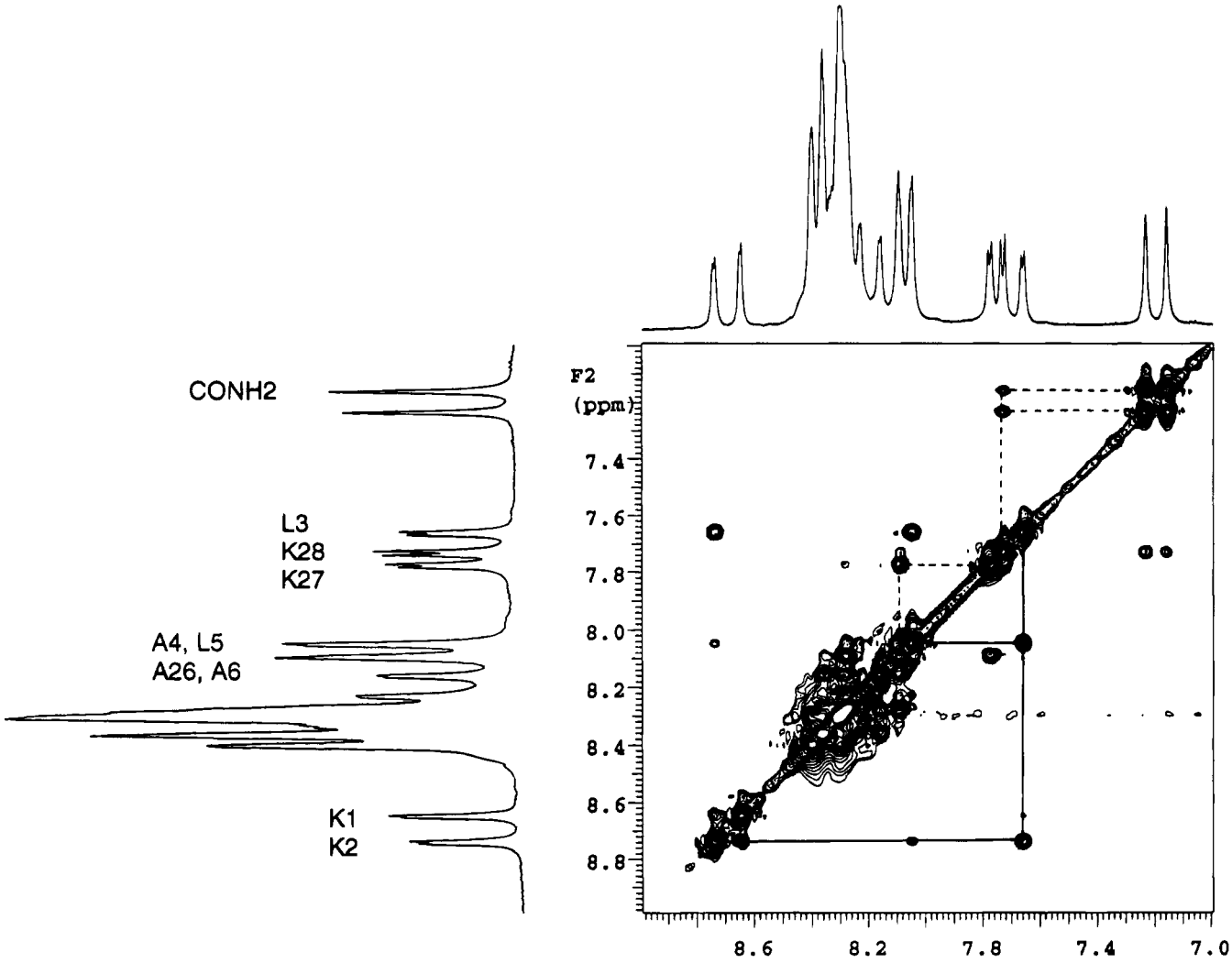

FIGURE 9: Two-dimensional NMR spectrum showing NOESY connectivities between the amide proton resonances of $(LA)_{12}$ in methanolic solution. Data were acquired in methanolic solution at 25 °C using a 200 ms mixing time. Positionally assigned amino acid residues giving rise to the amide resonances are as marked in the figure. The solid and dashed lines trace NOE connectivities between succesive amides at the N- and C-termini, respectively.

overlap. However, with this peptide there is a relatively good separation of resonances in the amide proton region, and this enabled the unique identification of the ^1H resonances of about 10 specific amino acid residues, whereas the remaining resonances could only be identified by residue type. The latter was established in a TOCSY experiment which relays magnetization from the amide proton along the amino acid side chain (Figure 8). Identification is established on the basis of the characteristic frequencies of the crosspeaks which are very different for lysine, alanine, and leucine residues (Wüthrich, 1986). The amide resonance at 7.67 ppm, for example, is identified as a leucine amide because of its connectivity to a side chain methyl resonance at 0.95 ppm. Sequential assignment of several of the amide protons was established in a NOESY experiment, which relies on interactions between protons that are close together in space. In α-helical peptides, for example, the short distance between successive amide protons (2.8 Å) leads to strong crosspeaks in the amide proton region. With $(LA)_{12}$, the NOESY spectrum is quite crowded because of the resonance overlap problems noted earlier. Despite this, however, a number of NH to NH contacts were observed among the more well-resolved resonances (see Figure 9). Indeed, as illustrated in Figure 9, the data are sufficiently well resolved to enable the tracing of two distinct sequences involving the lysine residues at the ends of the peptide. These two sequences, Lys-Lys-Leu-Ala and Ala-Lys-Lys, identify the N- and C-termini, respectively, because of the uniqueness of the sequences in those regions of the peptide. The assignment of the C-terminal amide protons was confirmed by the observation of NOESY crosspeaks from one of the lysine amides to the C-terminal primary amide blocking group at long mixing times. Such observations constitute the basis of the sequence-specific assignments that are summarized in Table 2. The results summarized therein indicate that the well-resolved amide protons all belong to the fast exchanging group, whereas most of the poorly resolved amide protons belong to the slowly exchanging group identified earlier. One should note, however, that despite the relatively fast rates of amide hydrogen exchange observed near the N- and C-termini of $(LA)_{12}$, the very existence of strong NOE connectivities between successive amides in those regions of the peptide is itself strongly supportive of the formation of helical structures in those regions. Thus, the relatively fast rates of amide exchange observed at the $(LA)_{12}$ termini do not necessarily imply the loss of helical structure in those regions. These observations greatly facilitate analysis of the amide exchange data.

Upon reexamination of the amide hydrogen exchange data in the light of the identity and positional data listed in Table 2, the following conclusions can be made. First, the fast exchanging population(s) of amide protons are all located close to the N- and C-termini of the peptide. The NMR data indicate that fast H/D exchange occurs primarily with the amide protons of the 6−8 amino acid residues located at each end of the peptide. Indeed, the data suggest that amide proton H/D exchange rates decrease progressively with progress from amino acid residues located at the ends to those located in the central region of the peptide. This conclusion is consistent with a picture in which $(LA)_{12}$ adopts a stable helical structure with so-called "frayed ends" when dissolved in methanol. Second, under the conditions of our NMR experiments, amide protons arising from Lys-1, Lys-2, and Leu-3 are almost completely exchanged within 5 min of dissolving $(LA)_{12}$ in CD_3OD, whereas those arising from Ala-26, Lys-27, and Lys-28 remain detectable (albeit at reduced intensity) for the first 10−15 min of the experiment (see Figure 6). Thus, within the fast exchanging population of amide protons, those originating from amino acid residues located close to the N-terminus exchange at faster rates than do those arising from amino acid residues located at or near to the C-terminus. This result can be explained by the fact that amido N−H bonds of helical peptides/proteins are directed toward the N-terminus of the helix. Thus, if one assumes that $(LA)_{12}$ is helical, then the amido protons arising from the first four amino acid residues at the N-terminus will not be involved in hydrogen-bonding interactions within the helix whereas the opposite is the case with amido protons arising from the last four amino acid residues at the C-terminus. Hence, given that the hydrogen-bonded amido protons are expected to exchange at a slower rates than would their nonbonded counterparts (Englander & Kallenbach, 1984), the differential rates of N−D exchange at the N- and C- termini can be attributed to simple geometrical effects consistent with $(LA)_{12}$ retaining a helical structure in methanolic solution. This result is significant because it implies that the two C-terminal lysine residues form part of the helical structure which $(LA)_{12}$ adopts in methanolic solution, a conclusion which is consistent with the strong NOE connectivities observed between the amide proton resonances assigned to this region of the peptide (see above). The significance of the issues raised above and their overall relevance to the populations of rapidly and slowly exchanging amide protons which probably occur when $(LA)_{12}$ is dissolved or dispersed in the various media will be explored in the Discussion.

One-dimensional ^1H NMR spectra of $(LA)_{12}$ dissolved in perdeuterated SDS micelles were also recorded to gain insight into the nature of the rapidly and slowly exchanging populations of amide protons which may exist in a hydrated lipid environment and to determine whether (and the extent to which) data obtained in our studies of methanolic solutions of $(LA)_{12}$ could be extrapolated to hydrated lipid bilayers. Spectra A and B in Figure 10 show the amide proton resonances of the ^1H NMR spectra of $(LA)_{12}$ dispersed in chain-perdeuterated SDS micelles in D_2O and in water, respectively. When compared with the equivalent spectra acquired in CD_3OD and CD_3OH (Figure 10, spectra C and D, respectively), it is clear that in aqueous SDS micelles most of the high-resolution information observed in methanolic solution has been lost because of the broadening of

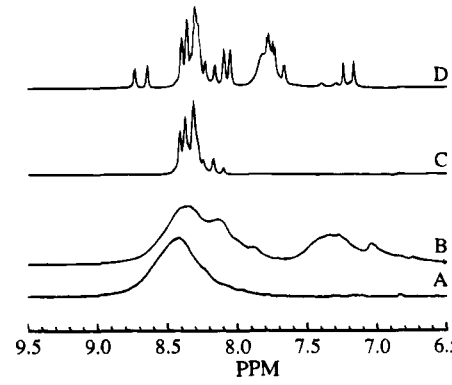

FIGURE 10: 500 MHz ^1H NMR spectra of $(LA)_{12}$ in methanolic solution and in aqueous SDS micelles. The data shown are the amide proton resonances of spectra obtained at 25 °C under the following conditions: (A) CD_3OH solution (1−1 solvent suppression). (B) CD_3OD solution after prolonged exposure to solvent. (C) SDS_{d25} micelles in water (1−1 solvent suppression). (D) SDS_{d25} micelles in D_2O.

the various resonances. This observation can be attributed to the slower tumbling rates (i.e., longer correlation times) of the larger peptide/SDS micellar particles compared to the peptide monomers. The spectra shown in Figure 10 indicate that amide D/H exchange also occurs in the SDS micelles and that rapidly and slowly exchanging populations can be clearly identified. Moreover, from a comparison of the chemical shift ranges of the rapidly exchanging amide protons observed in the aqueous and methanolic media, one can conclude that both rapidly exchanging populations of amide protons are located near the ends of the peptide chain. This observation is important because it indicates that one can extrapolate some information about the H/D exchangeability of the amide protons of $(LA)_{12}$ in methanolic solution to aqueous micellar aggregates.

Studies of the Intramembrane Orientation of Acetyl-$K_2(LA)_{12}K_2$-amide. The C=O stretching and amide I regions of the ATR-IR spectra of dried and hydrated films of $(LA)_{12}$/15:0 PC mixtures are shown in Figure 11. The dominant feature of the data shown is that when observed with the perpendicular polarized beam ($A_\perp$), the integrated intensity of the amide I absorption centered near 1656 cm^{-1} is considerably smaller than that observed with the parallel polarized beam ($A_\parallel$). For these samples our observations of the amide I absorption band yielded dichroic ratios (i.e., $A_\parallel$: $A_\perp$) near 1.75 ± 0.1 under virtually all conditions examined. This result was consistently obtained with $(LA)_{12}$/PC mixtures over a wide range of R_p. Under our conditions the perpendicularly polarized evanescent wave is aligned along the normal to the $x-y$ plane of the ATR crystal, and as a result our observations of amide I dichroic ratios that are significantly greater than unity are consistent with the transition dipole of the amide I absorption band (effectively the amide C=O bond stretching vector) being predominantly aligned at an acute angle to the normal of the $x-y$ plane of the crystal. Also, given that the amide C=O bond is usually aligned at an acute angle (<10°) to the long axis of the helix (Ghélis & Yon, 1982), these data suggest that the long axis of the $(LA)_{12}$ helix is itself aligned at an acute angle to the normal to the $x-y$ plane of the ATR crystal. Similar results (specifically the dichroic ratios) were obtained in parallel ATR-FTIR spectroscopic studies of L_{24}, the polyleucine analogue of $(LA)_{12}$ (data not shown).

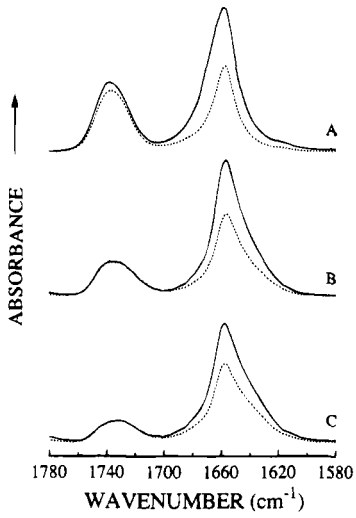

FIGURE 11: ATR-FTIR spectra of dried and hydrated $(LA)_{12}$ films. The absorbance spectra shown were obtained with the parallel ($A_{\parallel}$ solid lines) and perpendicularly polarized ($A_{\perp}$ dashed lines) beams for samples of the following: (A) Dried films of 15:0 PC/$(LA)_{12}$ mixtures (molar ratio = 10:1). (B) The gel phase of hydrated films of 15:0 PC/$(LA)_{12}$ mixtures (molar ratio = 10:1). (C) The liquid-crystalline phase of hydrated films of 15:0 PC/$(LA)_{12}$ mixtures (molar ratio = 10:1).

The CH_3 stretching and CH_2 stretching bands of the lipid hydrocarbon chains of the various samples indicate that in the gel phase the dichroic ratios of the lipid CH_3 symmetric stretching bands are consistently greater than unity, whereas those of the lipid CH_2 stretching bands are always less than unity (data not shown). Since the transition dipole of the CH_3 symmetric stretching band is aligned along the C−CH_3 bond (i.e., approximately 33° to the long axis of the lipid *all-trans* hydrocarbon chain), whereas that of the CH_2 stretching band is aligned nearly perpendicular to the long axis of the lipid *all-trans* hydrocarbon chain (Frengili & Günthard, 1981), the magnitudes of the dichroic ratios of the CH_3 symmetric stretching and CH_2 stretching absorption bands indicate that the long axes of the lipid *all-trans* hydrocarbon chains must themselves be aligned at an acute angle to the normal of the $x-y$ plane of the ATR crystal. These results indicate that the lipid bilayers are preferentially oriented on the surface of the ATR crystal and that the peptide $(LA)_{12}$ is oriented with the long axis of its predominantly helical structure essentially parallel to lipid bilayer normal. The implications of these data will be further explored in the Discussion.

DISCUSSION

Several important conclusions can be drawn from the spectroscopic data presented here. First, it is clear that essentially all of our data are consistent with $(LA)_{12}$ adopting a predominantly helical conformation whether dissolved in organic solvents, dispersed in aqueous lipid micelles, or incorporated into lipid bilayers. This conclusion was not unexpected given the amino acid sequence of $(LA)_{12}$, specifically the high α-helix forming propensities of leucine and alanine, and is strongly supported by the results of our CD and NMR spectroscopic experiments. Our FTIR spectroscopic data are also consistent with $(LA)_{12}$ containing a high percentage of α-helical structures but also suggest that under some circumstances significant amounts of non-α-helical structures may exist. For example, our analyses of the conformationally sensitive amide I band of $(LA)_{12}$ consistently indicate that whether dried from organic solvents or incorporated into hydrated lipid membranes, amide I absorptions assigned to α-helical domains of the peptide account for at least 70% of the total integrated intensity of the amide I band. However, when dissolved in methanol or in TFE, $(LA)_{12}$ populations (and/or domains) of seemingly nontrivial size (up to 35% of the integrated intensity of the amide I band) adopt a conformation that absorbs infrared radiation at frequencies between 1633 and 1638 cm^{-1}. The FTIR spectroscopic data also indicate that nontrivial amounts of this conformational form of the peptide are also formed when $(LA)_{12}$ is dispersed in 16:0 lyso-PC at low temperatures and under a variety of other conditions. Currently, the conformational basis of this absorption band is unknown. However, given that neither the CD nor NMR spectroscopic results reported here show any evidence for the formation of nonhelical structures under our experimental conditions, it seems unlikely that this band (and indeed the other unassigned absorption band between 1665 and 1680 cm^{-1}) could be originating from nonhelical domains and/or populations of $(LA)_{12}$. Also, considering that neither the CD nor the NMR spectroscopic methods used can easily differentiate between different helical forms of a protein or peptide nor, indeed, are they sufficiently sensitive to differentiate between distorted variations of these helical forms, we suggest that the unassigned amide I absorption bands alluded to above may arise from other helical forms or, possibly, from distorted forms of α-helical structures. Interestingly, it was recently demonstrated that short alanine-based peptides may exhibit a greater propensity to form 3_{10}-helices than α-helices in aqueous solution (Miick *et al.*, 1992; Fiori *et al.*, 1993). These authors showed that although the CD spectra of a number of alanine-based peptides were consistent with their adopting predominantly α-helical conformations, the FTIR spectra of these peptides were inconsistent with such a conclusion. These workers also presented strong electron spin resonance spectroscopic evidence that these alanine-based peptides may be forming 3_{10}-helices in aqueous solution (Miick *et al.*, 1992). Interestingly, the FTIR spectra of these alanine-based peptides exhibit a strong amide I absorption band near 1637 cm^{-1}, a frequency that is close to that observed in the present study. This observation suggests that the $(LA)_{12}$ IR absorption band near 1637 cm^{-1} may be originating from domains and or populations of the peptide which adopt 3_{10}-helical conformations under our experimental conditions. That $(LA)_{12}$ may adopt helical conformations other than the α-helix suggests that its effective hydrophobic length and surface topology in lipid bilayers may be subject to change, especially when the hydrophobic thickness of the host lipid bilayer is varied. Such issues are addressed in the accompanying paper (Zhang *et al.*, 1995b).

Second, it is clear from our studies that the secondary structure of $(LA)_{12}$ is quite responsive to changes in the properties of the surrounding medium, in contrast to the polyleucine-based analogues such as P_{16} and P_{24}. Evidence supporting this conclusion was largely obtained from our FTIR spectroscopic studies, which indicate that when $(LA)_{12}$ is dispersed in 16:0 lyso-PC, a marked reversible change in the contours of the amide I band occurs at temperatures where this lipid undergoes its micellar to coagel phase

transition. Since the so-called coagel phase of 16:0 lyso-PC is a chain-interdigitated lamellar structure for which the maximal hydrophobic thickness is equivalent to that of a single, fully extended hydrocarbon chain [see Huang and Mason (1986) and references cited therein], a substantial decrease in the effective hydrophobic thickness of the 16:0 lyso-PC assembly will occur at its micellar to coagel phase transitions. Thus, the observed changes in the $(LA)_{12}$ amide I band which accompany the micellar to coagel phase transition may well be the result of a significant change in peptide conformation in response to a drastic change in the thickness of the hydrophobic medium in which the peptide was embedded. Interestingly, the observed spectroscopic changes closely resemble those which occur when D_2O dispersions of $(LA)_{12}$ are cooled to similar temperatures (see Figures 3 and 6). This observation seems to bring into question the issue of whether the sample examined was simply an aqueous suspension of the peptide amongst micelles of 16:0 lyso-PC as opposed to being actually incorporated into the lyso-PC micelles. However, the former possibility seems unlikely because the rates of amide H/D exchange observed in D_2O and in 16:0 lyso-PC clearly differ (see Figure 5) and because the coagel to micellar phase transition of $(LA)_{12}$/16:0 lyso-PC mixture differs from that of the pure lyso-PC (data not shown). We suspect that the D_2O-suspended and lyso-PC-dispersed samples of $(LA)_{12}$ become more spectroscopically similar at temperatures below the micellar to coagel phase transition temperature of the lysolipid, because the drastic decrease in the hydrophobic thickness of the lysolipid assembly will expose a large fraction of the peptide to the aqueous medium. It is also noteworthy that comparable changes are not observed at the lamellar gel to lamellar liquid-crystalline phase transition of DPPC. Presumably this is because the mean hydrophobic thicknesses of the gel and liquid-crystalline lamellar phases of DPPC greatly exceed that of the coagel phase 16:0 lyso-PC.

Our studies of the exchangeability of the amide hydrogens of $(LA)_{12}$ also yielded useful insights into aspects of the conformational stability of this peptide, especially when these results are compared with similar studies previously performed on the polyleucine analogue (Zhang *et al.*, 1992a). It is evident that amide H/D exchange proceeds at a faster rate, and to a greater extent, with $(LA)_{12}$ than with the polyleucine-based analogue, indicating that the helical regions of $(LA)_{12}$ are considerably less stable to local secondary structure distortions and/or deformations that are likely to enhance amide proton exchange. As previously reported for the P_{24} model system, the observed rates of amide H/D exchange seem to define two distinct populations of amide protons which exchange with the bulk solvent at markedly different rates. In this study, high-resolution ^1H NMR spectroscopy enabled us to unequivocally determine that the rapidly exchanging population of amide protons are located near to the N- and C-termini of the peptide and to demonstrate that the rates of amide H/D exchange decrease markedly as one progresses from the free ends of the peptide toward the centrally located amino acid residues. Similar conclusions were made in our previous FTIR spectroscopic studies of the polyleucine-based peptide model P_{24} (Zhang *et al.*, 1992a). These results are compatible with the suggestion that even very stable peptide helices exhibit frayed termini (Nakanishi *et al.*, 1972).

As was observed our previous studies of the P_{24} peptide model (Zhang *et al.*, 1992a), the size of the slowly exchanging amide proton population of $(LA)_{12}$ varies with the composition of the medium in which the peptide was dispersed. Moreover, with $(LA)_{12}$ the relative sizes of its rapidly exchanging amide proton populations are generally larger than those observed with P_{24} under comparable conditions. This observation is consistent with $(LA)_{12}$ adopting a more deformable (or less conformationally stable) helical structure than P_{24}. However, an exception to this general observation seems to occur when $(LA)_{12}$ is dispersed in DPPC bilayers. Under these conditions the size of the rapidly exchanging amide proton population of $(LA)_{12}$ is smaller than that observed in deuterated organic solvents, the amide H/D exchange rates of the slowly exchanging population are slow enough to be deemed virtually unexchangeable, and the relative size of the latter population are generally comparable to, though slightly smaller than, that observed with similar preparations of P_{24}. These observations can be rationalized by suggesting that the hydrophobic core of the lipid bilayer inhibits H/D exchange by limiting the access of water to the central helical domains of both peptides. Alternatively, the hydrophobic core of the lipid bilayer may stabilize the helical conformation of both peptides and reduce the fraying of their termini.

Another consideration which is critical to the proposed use of this peptide as a model of the hydrophobic transmembrane helix pertains to the way in which the peptide orients when it is incorporated into a lipid bilayer. Our ATR-FTIR studies of macroscopically oriented lipid/peptide mixtures show that the dichroic ratio of the amide I absorption band is approximately 1.75, indicating that the long axes of the peptide helices are predominantly oriented normal to the bilayer plane. In principle, the ATR-FTIR data obtained here can be quantitatively analyzed to obtain an angular alignment of the amide I transition moment relative to its axis of reorientation, the bilayer normal [for details, see Fringeli and Günthard (1981) and Hübner and Mantsch (1990, 1991)]. However, such analyses implicitly assume that the lipid bilayers systems studied are uniformly and perfectly macroscopically oriented, and we do not have any independent evidence that such was the case with the samples studied. However, if one were to make such an assumption and further assume that the orientational order parameters of the amide I transition moment are near 0.7 [typical values for samples of this type, see Hübner and Mantsch (1990, 1991)], then the dichroic ratios measured under our conditions would be consistent with an orientation of the amide I transition dipoles of $(LA)_{12}$ and its polyleucine analogue being within 25° of the axis of reorientation. Interestingly, this value is comparable to that estimated in X-ray diffraction studies of oriented DPPC/P_{24} bilayers (Huschilt *et al.*, 1989). Since the degree of alignment of the peptide with the bilayer normal may indeed be higher that indicated above (because of imperfect orientation of the bilayers), these data provide strong evidence for $(LA)_{12}$ inserting into and traversing the lipid bilayer.

In conclusion, the peptides L_{24} and $(LA)_{12}$ were designed to insert into lipid bilayers as hydrophobic single-stranded transmembrane helices oriented with their long axes along the bilayer normal and with their polar N- and C-terminal capping residues anchored in the polar domains of the opposing lipid monolayers. However, unlike the first

generation polyleucine-based peptide models which adopt stable α-helical conformations which are not particularly sensitive to the physical properties of the lipid bilayers into which they are intercalated (Zhang *et al.*, 1992a,b, 1995a), $(LA)_{12}$ was designed such that it would assume a more "deformable" helical structure that should be more conformationally responsive to changes in the physical properties of host lipid bilayers. All of our spectroscopic data are consistent with $(LA)_{12}$ meeting the aforementioned design specifications, and thus studies of the interaction of this peptide with lipid bilayers should provide valuable insights into the way(s) in which hydrophobic helices can affect and can be affected by the physical properties of the lipid bilayers into which they are incorporated. The results of our differential scanning calorimetric and FTIR spectroscopic studies of the interaction of $(LA)_{12}$ with a homologous series of *n*-saturated diacyl-PCs which are presented in the following paper (Zhang *et al.*, 1995b).

ACKNOWLEDGMENT

We are indebted to Paul Semchuk and Len Daniels for the synthesis, purification, and analytical verification of the peptides L_{24} and $(LA)_{12}$, to Kim Oikawa for performing the CD measurements, and to Drs. Henry H. Mantsch and Michael Jackson of the Institute for Biodiagnostics at the National Research Council of Canada (Winnipeg, MB) for the availability of time on the Digilab FTS-60 FTIR spectrometer and for their assistance in performing the ATR-FTIR spectroscopic experiments.

REFERENCES

Bax, A., & Davis, D. G. (1985) *J. Mag. Reson. 65*, 355−360.
Chang, C. T., Wu, C.-S., & Yang, J. T. (1978) *Anal. Biochem. 91*, 13−31.
Chen, Y.-H., Yang, J. T., & Chau, K. H. (1974) *Biochemistry 13*, 3350−3359.
Chirgadze, Y. N., Brazhnikov, E. V., & Nevskaya, N. A. (1976) *J. Mol. Biol. 102*, 781−792.
Cserháti, T., & Szögyi, M. (1991) *Int. J. Biochem. 23*, 131−145.
Cserháti, T., M. Szögyi, M. (1992) *Int. J. Biochem. 24*, 525−538.
Cserháti, T., & Szögyi, M. (1993) *Int. J. Biochem. 25*, 123−146.
Cserháti, T., & Szögyi, M. (1994) *Int. J. Biochem. 26*, 1−18.
Davis, J. H., Clare, D. M., Hodges, R. S., & Bloom, M. (1983) *Biochemistry 22*, 5298−5305.
Dempsey, C. E. (1988) *Biochemistry 27*, 6893−6901.
Dwivedi, A. M., & Krimm, S. (1984) *Biopolymers 23*, 923−943.
Epand, R. M., & Epand, R. F. (1992) in *The Structure and Function of Biological Membranes* (Yeagle, P., Ed.) pp 573−601, CRC Press, Boca Raton.
Englander, S. W., & Kallenbach, N. R. (1984) *Quart. Rev. Biophys. 16*, 521−655.
Fiori, W. R., Miick, S. M., & Millhauser, G. L. (1993) *Biochemistry 32*, 11957−11962.
Fringeli, U. P., & Günthard, H. H. (1981) in *Membrane Spectroscopy* (Grell, E., Ed.) pp 270−332. Springer-Verlag, New York.
Ghélis C., & Yon, J. (1982) *Protein Folding*, Academic Press, New York.
George, R., Lewis, R. N. A. H., Mahajan, S., & McElhaney, R. N. (1989) *J. Biol. Chem. 264*, 11598−11604.
George, R., Lewis, R. N. A. H., & McElhaney, R. N. (1990) *Biochem. Cell Biol. 68*, 161−168.
Henry, G. D., & Sykes, B. D. (1994) *Methods Enzymol. 239*, 515−535.
Hore, P. J. (1983) *J. Mag. Reson. 55*, 283−300.
Huang, C., & Mason, J. T. (1986) *Biochim. Biophys. Acta 864*, 423−470.
Hübner, W., & Mantsch, H. H. (1990) in *Surfactants in Solution* (Mittal, K. L., & Shah, D. O., Eds.) Vol. 11, pp 303−314, Plenum Press, New York.
Hübner, W., & Mantsch, H. H. (1991) *Biophys. J. 59*, 1261−1272.
Huschilt, J. C., Hodges, R. S. & Davis, J. H. (1985) *Biochemistry 24*, 1377−1386.
Huschilt, J. C., Millman, B. M., & Davis, J. H. (1989) *Biochim. Biophys. Acta 979*, 139−141.
Jacobs, R. E., & White, S. H. (1986) *Biochemistry 25*, 2605−2612.
Jacobs, R. E., & White, S. H. (1987) *Biochemistry 26*, 6127−6137.
Lewis, R. N. A. H., Mak, N., & McElhaney, R. N. (1987) *Biochemistry 26*, 6118−6126.
Mantsch, H. H., Madec, C., Lewis, R. N. A. H., & McElhaney, R. N. (1985) *Biochemistry 24*, 2440−2446.
McElhaney, R. N. (1982) in *Current Topics in Membranes and Transport* (Razin, S., & Rottem, S., Eds.) Vol. 17, pp 317−380, Academic Press, New York.
McElhaney, R. N. (1986) *Biochim. Biophys. Acta 864*, 361−421.
McElhaney, R. N. (1994) in *Treatise on Biomembranes* (Lee, A. G., Ed.) Vol. 6, JAI Press, Greenwich, CT.
McLean, L. R., Hagaman, K. A., Owen, T. J., & Krstenansky, J. L. (1991) *Biochemistry 30*, 31−37.
Miick, S. M., Martinez, G. V., Fiori, W. R., Todd, A. P., & Millhauser, G. L. (1992) *Nature 359*, 653−655.
Miyazawa, T., & Blout, E. R. (1961) *J. Am. Chem. Soc. 83*, 712−719.
Morrow, M. R., Huschilt, J. C., & Davis, J. H. (1985) *Biochemistry 24*, 5396−5406.
Nakanishi, M., Tsuobi, M., Ikegami, A., & Kanehisa, M. (1972) *J. Mol. Biol. 64*, 363−378.
Papahadjopoulos, D., Moscarello, M., Eylar, E. H., & Isac, T. (1975) *Biochim. Biophys. Acta 401*, 317−335.
Pauls, K. P., MacKay, A. L., Söderman, O., Bloom, M., Tanjea, A. K., & Hodges, R. S. (1985). *Eur. Biophys. J. 12*, 1−11.
Rabolt, J. F., Moore, W. H., & Krimm, S. (1977) *Macromolecules 10*, 1065−1074.
Roux, M. R., Neumann, J. M., Hodges, R. S., Devaux, P. F., & Bloom, M. (1989) *Biochemistry 28*, 2313−2321.
Sandermann, H. (1978) *Biochim. Biophys. Acta 515*, 209−237.
Selinsky, B. S. (1992) in *The Structure and Function of Biological Membranes* (Yeagle, P., Ed.) pp 603−651, CRC Press, Boca Raton, FL.
Sengupta, P. K., & Krimm, S. (1985) *Biopolymers. 24*, 1479−1491.
States, D. J., Haberkorn, R. A., & Ruben, D. J. (1982) *J. Mag. Reson. 48*, 286−296.
Surewicz, W. K., & Mantsch, H. H. (1989) *Biochim. Biophys. Acta 952*, 115−130.
Watts, A., & De Pont, J. J. H. H. M., Eds. (1985) *Progress in Lipid Protein Interactions*, Vol. 1, Elsevier, Amsterdam.
Watts, A., & De Pont, J. J. H. H. M., Eds. (1986) *Progress in Lipid Protein Interactions*, Vol. 2, Elsevier, Amsterdam.
Wishart, D. S., Sykes, B. D., & Richards, F. M. (1991) *J. Mol. Biol. 222*, 311−333
Wüthrich, K. (1986) *NMR of Proteins and Nucleic Acids*, John Wiley & Sons, New York.
Zhang, Y.-P., Lewis, R. N. A. H., Hodges, R. S., & McElhaney, R. N. (1992a) *Biochemistry 31*, 11572−11578.
Zhang, Y.-P., Lewis, R. N. A. H., Hodges, R. S., & McElhaney, R. N. (1992b) *Biochemistry 31*, 11579−11588.
Zhang, Y.-P., Lewis, R. N. A. H., Hodges, R. S., & McElhaney, R. N. (1995a) *Biophys. J.* (in press).
Zhang, Y.-P., Lewis, R. N. A. H., Hodges, R. S., & McElhaney, R. N. (1995b) *Biochemistry 34*, 2362−2371.

BI942186I